

Fangfang LI^{1,2}¹ *National Aerospace University “Kharkiv Aviation Institute”, Ukraine*² *Key Laboratory of Nondestructive Testing (Ministry of Education),
Nanchang Hangkong University, Nanchang, China*

ADAPTIVE TWO-STEP METHOD FOR PROVIDING THE DESIRED VISUAL QUALITY FOR SPIHT

*Lossy compression has been widely used in various applications due to its variable compression ratio. However, distortions are introduced unavoidably, and this decreases the image quality. Therefore, it is often required to control the quality of the compressed images. A two-step method has been proposed recently to provide the desired visual quality. The average rate-distortion curve was used to determine the proper parameter value that controls compression. However, its performance for the wavelet-based coder Set Partitioning in Hierarchical Trees (SPIHT) is insufficient because there are very wide limits of visual quality variation for different images for a given value of the compression control parameter (CCP). Additionally, previous work has demonstrated that the level of errors, which is the subject of our study relates to texture features of an image to be compressed, where texture presence is an inherent property of remote sensing images. In this paper, our goal is to develop an adaptive two-step method for SPIHT to improve accuracy. The following tasks were solved. First, a prediction of visual quality for a particular parameter value is conducted. The prediction scheme is based on the information extraction from a certain number of image blocks to perform a visual quality calculation of the image compressed for a given CCP value. A threshold is adopted as the complexity grouping; in this paper, images are divided into two groups: simple and complex images. Second, the results of the grouping determine the adaptive curve model adopted. Finally, a two-step compression method is applied according to this curve. The classical metric Peak signal-to-noise ratio (PSNR) is employed to evaluate the image quality. The research method is based on a validation experiment that is conducted for an image set covering different image complexity and texture features. The comparison results of four typical desired values prove that the accuracy has been generally improved, the variances of both the first and second steps have been reduced sufficiently, and the mean absolute error has also been improved. **Conclusion:** the improvement effects are significant, particularly in the low desired visual quality. A remote sensing image is taken as an example to analyze in detail; the quality of the decompressed images meets the user's visual requirement, and the errors are acceptable.*

Keywords: two-step approach; lossy compression; desired quality; adaptive curve model.

Introduction

Nowadays, images have become the most critical data in information recording and transmission with the development of imaging technology and the extensive use of various smart applications [1-3]. A dramatic increase in the size and volume of images is observed, which leads to the difficulty in data saving and transferring in conditions of a limited bandwidth of a communication line. Consequently, compression is the essential mean to reduce the size to save storage space and improve transmission efficiency.

In general, compression techniques can be divided into two categories, namely lossless and lossy, respectively [4, 5]. The latter is widely used since it produces higher compression ratio (CR) than the former. This is especially important for remote sensing

(aerial and satellite) images collected from platforms with limited storage resources and limited transmission bandwidth, such as airborne and spaceborne [6, 7].

However, the cost is that a certain degree of distortion will be introduced alongside high CR. Severe distortion results in the decompressed images' poor quality and affects further processing or visual perception. Therefore, like CR, image quality is also an important factor in lossy compression and should even be considered as a priority in many cases [8-10]. If the terminal is a human, noticeable distortions will be visible and affect the visual perception [1, 11]; if the decompressed images need to be processed by machine algorithms, poor quality negatively influences the object estimation accuracy or probability of correct classification [12-14]. In these conditions, it is necessary to control the distortions within a certain range.

Generally, CR increase is accompanied by image quality decrease, and vice versa; it is determined by compression control parameter (CCP), adopted coder and image features [12, 15-17]. The essential part of controlling the distortions is setting the proper CCP for a compressed image in lossy compression according to quality requirements. Concerning this task, the earlier contributions were from two aspects. The first is providing the desired quality through the iterative method. In [18], the formulation of 2D Discrete Cosine Transform (DCT) coefficient and iterative JPEG2000 encoding scheme was proposed to control the quality of a reconstructed image. The second is based on prediction of quality based on the chosen statistical parameter. In [19], a deep learning-based picture-wise just noticeable difference prediction model was proposed for lossy compression according to the perceptually lossy/lossless predictor results.

A two-step compression method has been proposed recently, which avoids the multi-iteration to improve time efficiency and correct the parameter in terms of the initial quality of the first step compression to reduce the error [20-22]. Given this, the two-step method outperforms the existing distortion control methods. Our previous works have proved that this method works well for the DCT-based coder AGU and HEVC-based coder BPG [21-23], and its adaptive version reduces the errors for the metric PSNR [24]. However, the accuracy of providing a desired quality for the Discrete Wavelet Transform (DWT)-based coder Set Partitioning in Hierarchical Trees (SPIHT) is insufficient sometimes [25] because of several reasons that will become clear after more detailed analysis.

The goal of this paper is to propose and study the adaptive two-step method for the SPIHT coder and to further improve its accuracy. It is confirmed by the validation experiment that pre-classification of image complexity helps to choose the appropriate curve model and does improve the results in terms of PSNR, which had large errors in our previous works.

The rest of this paper is organized as follows. Positive features of SPIHT are described in Section 1. The basics of the two-step method applied to SPIHT are defined in Section 2. Adaptation strategy is described in Section 3. The experiment validation is presented in Section 4. The discussion is given in Section 5. Finally, Section 6 summarizes the work and provides conclusions.

1. Peculiarities and applications of SPIHT

SPIHT [26] is known to be one of popular methods of lossy image compression. It uses wavelet decomposition of an image to be compressed and

inherent similarities across the sub-bands. The most important wavelet coefficients are coded in the first order. Due to this, similarly to the later introduced standard JPEG2000, several positive features are provided. First, progressive compression can be provided. Second, a desired compression ratio can be ensured. Third, better performance compared to JPEG in terms of traditional quality metrics as mean square error (MSE) or peak signal-to-noise ratio (PSNR) is usually achieved. In addition, SPIHT is rather fast and can be freely used. These advantages can be extremely useful if the main requirements to image compression method and algorithm stem from the desire to transfer a compressed image via a band-limited communication link within a given time.

The aforementioned properties explain the wide use of SPIHT in practice. For example, SPIHT application for lossy compression of medical images in magneto-resonance and computer tomography systems is considered in the papers [27, 28]. The use of different modifications is analyzed by many researchers. In particular, the use of different wavelets is studied in [28], the authors of [29] consider the use of Burrows-Wheeler transform within the SPIHT framework in attempts to improve general performance of the SPIHT coder.

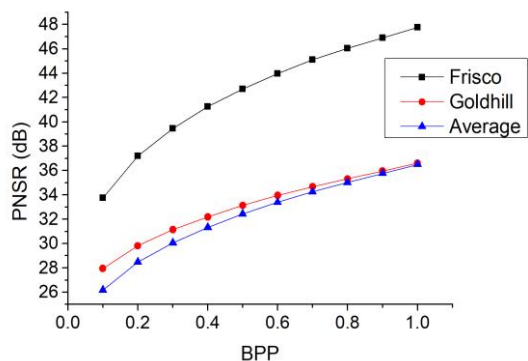
Performance of SPIHT is mostly analyzed in terms of conventional quality metrics as MSE or PSNR. Meanwhile, there is an obvious tendency to using visual quality metrics including combined ones [30]. However, even for the conventional metrics, there are certain problems for SPIHT if it is desired to provide not a given CR, but a desired quality. For a given CR or bits per pixel (BPP), quality of images compressed by SPIHT (as well as by many other compression techniques) vary in very wide limits (see data in [25], the examples will be given in Section 2). Then, by setting some fixed BPP, it is difficult to provide a desired quality for any image to be compressed and one has to carry out adaptation to image content [25]. Such an adaptation can be done in different ways where the two-step method proposed in [25] and further called as basic is one of them. This method is fast (since it is based on two compressions and one decompression) but, for certain practical situations, it is not accurate enough. Thus, below we discuss how the accuracy can be improved.

2. Review of basic two-step method on SPIHT

The basic two-step method of image compression consists of two main stages. The first one is preliminary image compression/decompression with the initial CCP determined by the average rate-distortion curve obtained

off-line (in advance). The second compression stage is conducted with the recalculated CCP referring to image quality feedback in the first step. This approach is based on several assumptions. The first assumption is that rate-distortion curves behave similarly and particular rate-distortion curves for all images do not differ a lot from the aforementioned averaged rate/distortion curve obtained in one or another way. The second assumption is that the rate/distortion curves are monotonous functions for all images and these functions can be quite accurately approximately linearly, i.e., using only the first derivative where derivative values for particular rate/distortion curves are supposed to be quite close to that one for the average curve for the same CCP. If these assumptions do not hold, the method can fail in one or another way or, at least, its performance can radically worsen and become inappropriate.

In previous works, the result of applying the two-step method to SPIHT has occurred considerably less optimistic than for the DCT-based coder AGU [21, 25]. In particular, the largest residual errors of providing a desired metric value took place for simple structure images and/or low desired quality. The reason is that these images' rate-distortion curves differ a lot from the average one, which led to the inappropriate initial CCP and erroneous estimate of derivative used in calculation of the corrected CCP.



1. Dependences of PSNR on BPP for SPIHT

Fig.

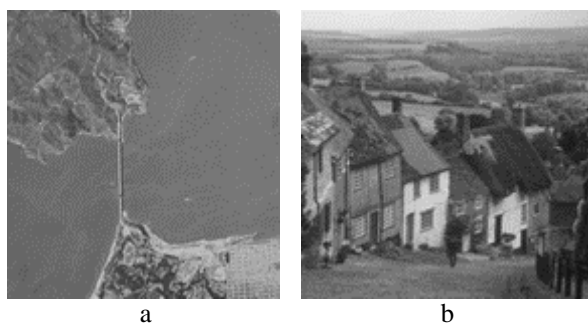


Fig. 2. Sample images: a) Frisco, b) Goldhill

curves are also presented for comparison and detailed analysis. The images are shown in Figure 2. The curve for the test image Goldhill is very similar to the average one; therefore, accuracy of quality provided by the conventional two-step method for this test image is high, the residual error is appropriate [25]. However, for the simple structure image Frisco (that contains large quasi-homogeneous regions), the rate/distortion curve differs a lot from the average curve. This results in the residual error that is the largest among the test images considered in [25]. Therefore, the accuracy is worth improving especially for simple structure images and low desired PSNR. The two-step compression method [25] requires simultaneous fast realization of both fast discrete wavelet and cosine transforms.

3. Adaptive two-step method on SPIHT

Aiming at the problem that the difference in image complexity results in the mismatch of the average rate-distortion curve, an adaptive method was proposed for AGU [24]. Because of its effective improvement, and thanks to the image quality prediction method proposed recently [31], it is possible to apply an adaptive two-step method to SPIHT.

The main idea consists in the following. We assume that it is possible to easily, reliably and quickly pre-classify an image to be compressed and refer it to two (or even more) classes (categories). Having average rate/distortion curves for all classes and assuming that particular rate/distortion curves for images of a given class are close to the corresponding average rate/distortion curve, it is possible to set the initial (first step) CCP better and to use a better estimate of derivative in the second step.

In this study, we have limited ourselves by considering two classes. The average rate-distortion curves were obtained from two basic image sets. In this paper, all basic images were divided into simple and complex groups. The grouping was based on the image quality prediction value for a fixed CCP, bit per pixel (BPP) in the SPIHT coder [24, 31].

Let us briefly review the previous method of quality prediction for SPIHT. This prediction method is based on the fixed relationship between the dependence of the visual quality values of the coder SPIHT and discrete cosine transform (DCT) coder AGU [31].

$$PSNR_{SPIHT} = PSNR_{AGU} - 0.6232, \text{ dB.} \quad (1)$$

The average dependence curves of PSNR ($PSNR_{SPIHT}$ and $PSNR_{AGU}$) on CR for two coders are similar, and the deviation is basically fixed for each CR value. Then, the PSNR value for SPIHT can be

A part of average rate-distortion curve is given in Figure 1, two examples of particular rate/distortion

calculated as equation (1). The following algorithms are adopted to obtain the prediction result:

1) for a given BPP, the CR of SPIHT is determined by $CR \approx 8/BPP$ [25];

2) Then this CR value is utilized to calculate the P_{0q} for AGU according to equation (2), where the P_{0q} denotes the mean probability that quantized DCT coefficients in 8×8 blocks are equal to zero [32], calculated as equation (3);

$$CR = 0.9462 * \exp(2.895P_{0q}) + 1.045 * 10^{(-13)} \exp(35.52P_{0q}), \quad (2)$$

$$P_{0q} = \frac{\sum_{n=1}^{(N_{bl})} N_n}{(64N_{bl})}. \quad (3)$$

Here N_n denotes the number of DCT coefficients to be zeroed after quantization for an n -th block, N_{bl} denotes the number of the considered 8×8 pixel blocks randomly chosen in a considered image;

3) search for the proper QS value corresponding to the P_{0q} . First, set an initial value of QS, e.g., equal to 0, then gradually increase it until the percentage of DCT coefficients with absolute values smaller than $QS/2$ is smaller than P_{0q} ;

4) predict the PSNR for AGU according to the following equations

$$D_q(n, k, l) = \left[\frac{D(n, k, l)}{QS} \right], k = 0, \dots, 7; l = 0, \dots, 7; \quad (4)$$

$$\Delta D_q(n, k, l) = QS * D_q(n, k, l) - D(n, k, l), k = 0, \dots, 7; l = 0, \dots, 7; \quad (5)$$

$$MSE = \frac{1}{N} \sum_{n=1}^N MSE_n = \quad (6)$$

$$= \frac{1}{64N} \sum_{n=0}^N \sum_{k=0}^7 \sum_{l=0}^7 \Delta D_q(n, k, l)^2;$$

$$PSNR = 10 * \log_{10}(MAX^2 / MSE), \quad (7)$$

where $D(n, k, l)$ denotes a set of DCT coefficient for an n -th block, $\Delta D_q(n, k, l)$ denotes the difference after quantification, MAX defines the image dynamic range;

5) plus the fixed average deviation on the prediction PSNR of the coder AGU as equation (1). Finally, the predicted PSNR for SPIHT is obtained.

This prediction approach described above provides an estimate value of PSNR for a given BPP using some calculation to replace the actual compression. The time consumption is about 2/3 of SPIHT compression, and the standard deviation of residual errors of providing a desired PSNR is about a few dB.

In this paper, the predicted value (7) is utilized to pre-classify an image to be compressed to two groups,

simple and complex structure ones. The BPP is given as 0.5, 300 8×8 random image blocks are chosen to calculate the prediction PSNR (7). The basic image set prediction results are shown in Figure 3.

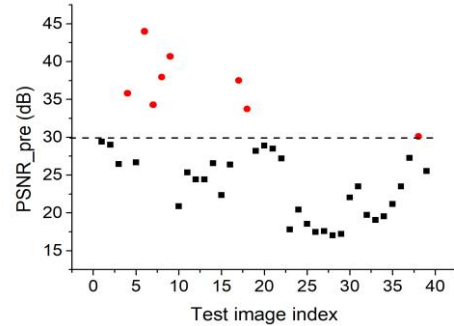


Fig. 3 Prediction of PSNR for SPIHT (BPP=0.5)

Let us set the $PSNR = 30$ dB as the threshold (Horizontal dotted line in Fig. 3); if the prediction PSNR is larger than 30 dB, then the image is treated as the simple one (marked as a red dot). Otherwise, it belongs to the complex image set (marked as a black square).

As we can see in Fig. 3, most images belong to the class of “complex structure images”. Only 7 out of 39 test images have been classified as simple structure ones.

The average curves drawn from images of two classes are shown in Figure 4. It can be seen from analysis of these curves that the average values for simple images are considerably (by 10-15 dB) higher than for the complex ones due to image different complexity.

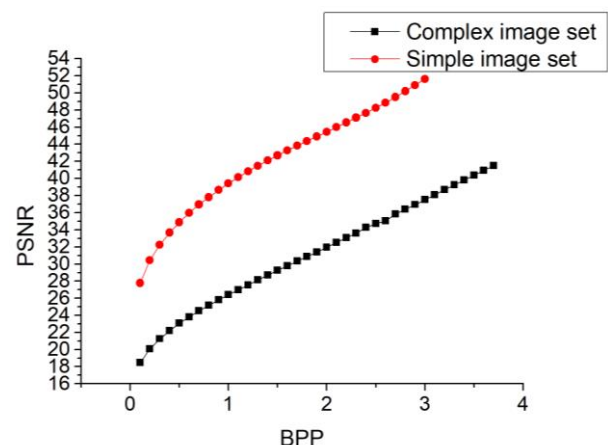


Fig. 4. Grouped dependences of PSNR on BPP for SPIHT

The proposed pre-classification approach is performed for each image to be compressed.

The considered image is automatically classified as simple or complex images; the average curve is chosen adaptively; the two-step method is implemented according to the following equations:

$$BPP_{init} = BPP_{est} + \frac{PSNR_{des} - PSNR_{ave}}{M'} ; \quad (8)$$

$$BPP_{des} = BPP_{init} + \frac{PSNR_{des} - PSNR_{init}}{M'} , \quad (9)$$

where BPP_{est} is the left margin of the adaptively chosen average rate/distortion interval, $PSNR_{ave}$ is the PSNR average distortion value corresponding to the BPP estimate. M' is the derivative corresponding to the BPP estimate, $PSNR_{init}$ is the decompressed image quality in the first step, BPP_{des} is corrected by equation (2) and used at the second step of compression.

4. Validation Experiment

Below we study the proposed method for SPIHT which has several known advantages like fast execution speed and wide application in lossy compression [15, 33]. The experiment has been conducted in three stages to verify its feasibility.

First, thirty-nine gray-scale images [34, 35] were chosen as the basic image set, including nine general-purpose images and thirty texture images, some of which are shown in Figure 5. This image set was divided into two groups, and then serial experiments have been conducted for each image and a wide range of BPP values; some of the data are shown in Table 1. Finally, the average rate-distortion curves (see Figure 4) have been obtained.

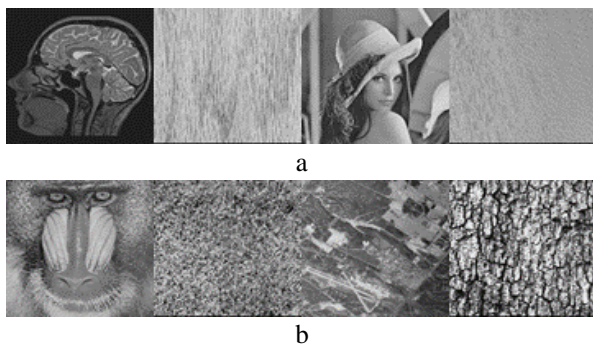


Fig. 5. Basic image sample: a) simple images, b) complex images

Second, twenty images [34, 35] have been chosen as the test image set to conduct the validation experiment with curve models from the basic image set. These test images have been also split into two groups with the same prediction and classification strategy used in the basic image set.

Some of images are presented in Figure 6.

Table 1
Dependence of PSNR (in dB) on BPP for SPIHT

Test image \ BPP	0.5	0.6
Mrt_prepared	38.211	38.742
Test8	36.317	37.323
Lenna	37.235	38.039
Test9	31.013	32.346
Baboon	25.628	26.497
Test1	20.881	21.584
Diego	26.632	27.271
Test15	20.373	21.088

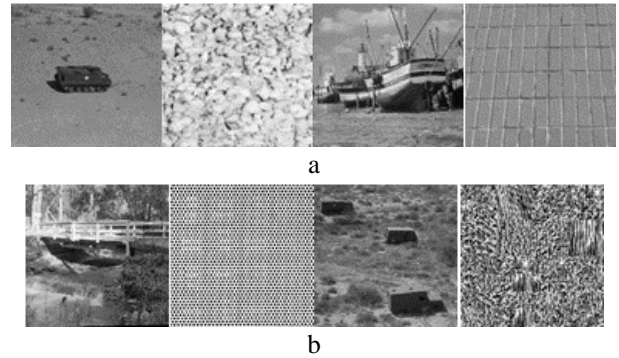


Fig. 6. Test image sample: a) simple images, b) complex images

Finally, an adaptive two-step method validation experiment has been implemented for two groups of images. Three typical values have been chosen for the metric PSNR, and the results are presented in the next section. For comparison, the results for the previous two-step method [25] for these test images have been obtained as well.

5. Discussion of the results

In this section, the experiment results are presented and comparatively analyzed. The results of the previous method are shown in Table 2, and the results for the adaptive method are given in Table 3, where the experiment was conducted for simple images and complex ones separately, but the data were combined into one Table to facilitate comparison.

In our study, four typical PSNR are chosen as the desired values, 40 dB, 35 dB, 32.5 dB, and 30 dB, respectively. These values roughly correspond to three levels of visual lossless, JDN distortions, visible distortion, and clearly visible distortion [21, 36].

For statistical analysis, the variances of image quality in the first and second steps have been calculated and denoted as VAR_{fir} and VAR_{sec} , respectively. The $MAX_{\Delta_{final}}$ denotes the maximum value

of errors for each group, and the MAE denotes the Mean Absolute Error for each group data.

Table 2

Statistic results for the basic method on test images

PSNR _{des} (dB)	VAR _{fir}	VAR _{sec}	MAXΔ _{final}	MAE
40	37.6386	1.9183	5.9907	0.5049
35	41.831	5.4447	5.5956	1.5911
32.5	45.0757	8.0088	6.4782	1.9306
30	48.7648	13.5432	7.9147	2.5726

Table 3

Statistic results for the adaptive method on test images

PSNR _{des} (dB)	VAR _{fir}	VAR _{sec}	MAXΔ _{final}	MAE
40	22.2946	2.4362	5.81	0.8618
35	24.4809	5.2552	4.7989	1.7228
32.5	19.9957	1.6254	4.76	0.6347
30	32.9900	2.0219	5.378	07799



a



b

Fig. 7. Remote sensing image example: a) original image, b) PSNR_{pro} = 40.708, CR = 4.086

From these data comparisons, it is proved that the adaptive scheme improves the overall accuracy of the two-step method for SPIHT lossy compression. First, the variances in the first step compression have been reduced sufficiently with the better initial CCP; second, the residual errors of visual quality providing are smaller and more convergent due to the adaptive selection of the average rate-distortion curve, which is more significant at a low desired quality (30 dB).



a



b

Fig. 8. Remote sensing image example:
 a) PSNR_{pro} = 33.944, CR = 7.160,
 b) PSNR_{pro} = 27.098, CR = 19.112

For a detailed analysis of the adaptive method on remote sensing images [37], one example is shown in Figures 7 and 8. The example image was compressed for the desired quality equal to 40 dB, 35 dB, and 30 dB, the original image and decompressed image with small CR are presented in Figure 7, a and 7, b, respectively. The image in Figure 6, b has an excellent

quality, which is indistinguishable from the original image. The image in Figure 8, a has a good quality, and the distortion is not easy to notice; the image in Figure 8, b has relatively bad quality, but it allows to understand the content of the image in spite of distortions that are mainly concentrated in texture/detail areas; meanwhile the high compression ratio (CR) is achieved. The example also shows that the largest residual error is observed for $PSNR_{des} = 30$ dB.

It is demonstrated that the proposed adaptive method for two-step compression is able to provide the desired quality for SPIHT coder. The user can set a proper desired value according to requirements for a given application, and achieve the highest CR.

6. Conclusions

In this study, we have presented an adaptive two-step method of providing the desired quality for the SPIHT coder to improve the accuracy. The proposed scheme employs different average rate-distortion curves for an image to be compressed depending on its complexity which is characterized by the prediction of the decompressed image corresponding to a fixed CCP. Experimental results have demonstrated the effectiveness of the proposed scheme especially if the desired quality is quite low according to PSNR. The pre-classification algorithm is fast and helps to improve the two-step method for the SPIHT coder.

Applicability of the proposed approach is demonstrated for one remote sensing image. Lossy compression of panchromatic remote sensing data is one possible area where the adaptive two-stage method can be useful taking into account wide limits of complexity variations of such images. In addition, image complexity can be analyzed for Y component of color and multispectral remote sensing data for compression of which SPIHT and its multichannel modifications are employed. Besides, it is expected that the adaptive version can be exploited for medical image compression especially when visually lossless compression is needed.

In the future, we expect that a simpler and faster image complexity algorithm can be found for the two-step method, and more refined adaptive curves will be employed to further improve the accuracy.

References (GOST 7.1:2006)

1. Zappavigna, M. *Social media photography: construing subjectivity in Instagram images [Text]* / M. Zappavigna // *Visual Communication*. – 2016. – Vol. 15, No. 3. – P. 271–292. DOI: 10.1177/1470357216643220.

2. *Simulation, image processing, and ultrasound systems for assisted diagnosis and navigation [Text]* / D. Stoyanov [et al]. – Cham : Springer, 2018. – 204 p. DOI: 10.1007/978-3-030-01045-4.

3. *Design of a high-performance system for secure image communication in the internet of things [Text]* / E. Kougianos [et al] // *IEEE Access*. – 2016. – Vol. 4. – P. 1222–1242. DOI: 10.1109/ACCESS.2016.2542800.

4. Sayood, K. *Introduction to data compression [Text]* / K. Sayood. – San Francisco : Morgan Kaufmann, 2017. – 768 p. ISBN: 978-0-12-415796-5.

5. Hussain, A. J. *Image compression techniques: A survey in lossless and lossy algorithms [Text]* / A. J. Hussain, A. Al-Fayadh, N. Radi // *Neurocomputing*. – 2018. – Vol. 300. – P. 44–69. DOI: 10.1016/j.neucom.2018.02.094.

6. Telles, J. *Multispectral Image Compression Algorithm for Small Satellites Based on Wavelet Subband Coding [Text]* / J. Telles, G. Kemper // *Smart Innovation, Systems and Technologies : Proc. of the 5th Brazilian Technology Symposium, Campinas, Brazil, 22-24 Oct., 2019. – Campinas, 2019. – P. 181–191. DOI: 10.1007/978-3-030-57548-9_17.*

7. Uchaev, Dm. V. *Theory and methodology of multifractal interpretation of aerospace images [Text]* / Dm. V. Uchaev, D. V. Uchaev // *Machine Vision (ICMV 2019) : Proc. of Twelfth International Conference, Amsterdam, Netherlands, 16-18 Nov., 2019. – Amsterdam, 2019. – P. 902–909. DOI: 10.1117/12.2559168.*

8. *Spectral distortion in lossy compression of hyperspectral data [Text]* / B. Aiazzi [et al] // *Journal of Electrical Computer Engineering*. – 2012. – Vol. 2012. – 8 p. DOI: 10.1155/2012/850637.

9. Ayoobkhan, M. U. A. *Lossy image compression based on prediction error and vector quantisation [Text]* / M. U. A. Ayoobkhan, E. Chikkannan, K. Ramakrishnan // *EURASIP Journal on Image Video Processing*. – 2017. – Vol. 2017, No. 1. – P. 1–13. DOI: 10.1186/s13640-017-0184-3.

10. *Flexible lossy compression for selective encrypted image with image inpainting [Text]* / C. Qin [et al] // *IEEE Transactions on Circuits Systems for Video Technology*. – 2019. – Vol. 29, No. 11. – P. 3341–3355. DOI: 10.1109/TCSVT.2018.2878026.

11. Grgic, M. *High-Quality Visual Experience: Creation, Processing and Interactivity of High-Resolution and High-Dimensional Video Signals [Text]* / M. Grgic, M. Kunt, M. Mrak. – Cham : Springer, 2010. – 561 p. ISBN-10: 3642128017.

12. *Effects of JPEG and JPEG2000 lossy compression on remote sensing image classification for mapping crops and forest areas [Text]* / A. Zabala [et al] // *Geoscience and Remote Sensing : Proc. of 2006 IEEE International Symposium, Denver, CO, USA, 31 July-4 Aug., 2006. – Denver, 2006. – P. 790–793. DOI: 10.1109/IGARSS.2006.203.*

13. Koschan, A. *Detection and classification of edges in color images [Text]* / A. Koschan, M. Abidi //

IEEE Signal Processing Magazine. – 2005. – Vol. 22, No. 1. – P. 64–73. DOI: 10.1109/MSP.2005.1407716.

14. Ozah, N. Compression improves image classification accuracy [Text] / N. Ozah, A. Kolokolova // *Proceedings of Canadian Conference on Artificial Intelligence*. – 2019. – Vol. 11489C. – P. 525–530. DOI: 10.1007/978-3-030-18305-9_55.

15. Satellite image remote sensing for identifying aircraft using SPIHT and NSCT [Text] / S. Doss [et al] // *IEEE Signal processing magazine*. – 2020. – Vol. 7, No. 5. – P. 631–634. DOI: 10.31838/jcr.07.05.130.

16. Oh, H. Visually lossless JPEG 2000 for remote image browsing [Text] / H. Oh, A. Bilgin, M. Marcellin // *Information*. – 2016. – Vol. 7, No. 3. – Article no. 45. DOI: 10.3390/info7030045.

17. Medical image compression based on region of interest using better portable graphics (BPG) [Text] / D. Yee [et al] // *Systems, Man, and Cybernetics (SMC) : Proc. of 2017 IEEE international conference, Banff, AB, Canada, 5-8 Oct., 2017. – Banff, 2017. – P. 216–221. DOI: 10.1109/SMC.2017.8122605.*

18. Quality controlled ECG data compression based on 2D discrete cosine coefficient filtering and iterative JPEG2000 encoding [Text] / A. Pandey [et al] // *Measurement*. – 2020. – Vol. 152. – Article no. 107252. DOI: 10.1016/j.measurement.2019.107252.

19. Deep learning-based picture-wise just noticeable distortion prediction model for image compression [Text] / H. Liu [et al] // *IEEE Transactions on Image Processing*. – 2019. – Vol. 29. – P. 641–656. DOI: 10.1109/TIP.2019.2933743.

20. Li, F. A Two-step Procedure for Image Lossy Compression by ADCTC With a Desired Quality [Text] / F. Li, S. Krivenko, V. Lukin // *Dependable Systems, Services and Technologies (DESSERT) : Proc. of 2020 IEEE 11th International Conference, Kyiv, Ukraine, 14-18 May, 2020. – Kyiv, 2020. – P. 307–312. DOI: 10.1109/DESSERT50317.2020.9125000.*

21. Li, F. A Two-step Approach to Providing a Desired Visual Quality in Image Lossy Compression [Text] / F. Li, S. Krivenko, V. Lukin // *Advanced Trends in Radioelectronics, Telecommunications and Computer Engineering (TCSET) : Lviv-Slavske, Ukraine, 25-29 Feb., 2020. – Lviv-Slavske, 2020. – P. 502–506. DOI: 10.1109/TCSET49122.2020.235483.*

22. Li, F. Analysis of two-step approach for compressing texture images with desired quality [Text] / F. Li, S. Krivenko, V. Lukin // *Авіаційно-космічна техніка і технологія*. – 2020. – № 1(161). – С. 50–58. DOI: 10.32620/akt.2020.1.08.

23. Li, F. An Approach to Better Portable Graphics (BPG) Compression with Providing a Desired Quality [Text] / F. Li, S. Krivenko, V. Lukin // *Advanced Trends in Information Theory (ATIT) : Proc. of 2020 IEEE 2nd International Conference, Kyiv, Ukraine, 25-27 Nov., 2020. – Kyiv, 2020. – P. 13–17. DOI: 10.1109/ATIT50783.2020.9349289.*

24. Li, F. Adaptive two-step procedure of providing desired visual quality of compressed image [Text] / F. Li, S. Krivenko, V. Lukin // *Electronic Information*

Technology and Computer Engineering : Proc. of the 2020 4th International Conference, Xiamen, China, 6-8 Nov., 2020. – Xiamen, 2020. – P. 407–414. DOI: 10.1145/3443467.3443791.

25. Li, F. Two-step providing of desired quality in lossy image compression by SPIHT [Text] / F. Li, S. Krivenko, V. Lukin // *Радіоелектронні і комп'ютерні системи*. – 2020. – № 2(94). – С. 22–32. DOI: 10.32620/reks.2020.2.02.

26. Said, A. A new, fast, and efficient image codec based on set partitioning in hierarchical trees [Text] / A. Said, W. Pearlman // *IEEE Transactions on Circuits and Systems for Video Technology*. – 1996. – Vol. 6, no. 3. – P. 243–250. DOI: 10.1109/76.499834.

27. Rao, G. S. Comparative Analysis of SVD and Progressive SPIHT techniques for Compression of MRI and CT Images [Text] / G. S. Rao, M. L. P. Rani, B. P. Rao // *International Conference on Sustainable Computing in Science, Technology & Management (SUSCOM-2019), Jaipur, India, Febr. 2019, Jaipur, 2019. – P. 521-529. DOI: 10.2139/ssrn.3352392.*

28. Kumar, B. B. S. Correlative Analysis of EZW and SPIHT Compression Algorithms using Sevenlets Wavelet Technique [Text] / B. B. S. Kumar, P. S. Satyanarayana // *International Journal of Innovative Technology and Exploring Engineering*. – 2020. – Vol. 9, no. 5. – P. 1099-1104. DOI: 10.35940/ijitee.e2672.039520.

29. Arunpandian, S. An effective image compression technique based on burrows wheeler transform with set partitioning in hierarchical trees [Text] // S. Arunpandian, S. S. Dhenakaran // *Concurrency and Computation. Practice and Experience*. – 2021. – Vol. 34, no. 5. – Article no. e6705. DOI: 10.1002/cpe.6705.

30. Ieremeiev, O. I. Combined Visual Quality Metric of Remote Sensing Images Based on Neural Network [Text] / O. I. Ieremeiev, V. V. Lukin, K. Okarma // *Radioelectronic and computer systems*. – 2020. – No. 4. – P. 4-15. DOI: 10.32620/reks.2020.4.01.

31. Li, F. A Fast Method for Visual Quality Prediction and Providing in Image Lossy Compression by SPIHT [Text] / F. Li, S. Krivenko, V. Lukin // *Integrated Computer Technologies in Mechanical Engineering–Synergetic Engineering: Proc. of Conference, Kharkov, Ukraine, 29-30 Oct., 2020. – Kharkov, 2020. – P. 17–29. DOI: 10.1007/978-3-030-66717-7_2.*

32. Prediction of visual quality metrics in lossy image compression [Text] / S. Krivenko [et al] // *Electronics and Nanotechnology (ELNANO) : Proc. of 2020 IEEE 40th International Conference, Kyiv, Ukraine, 22-24 April, 2020. – Kyiv, 2020. – P. 478–483. DOI: 10.1109/ELNANO50318.2020.9088819.*

33. Jamel, A. L. E. M. Efficiency Spiht in compression and quality of image [Text] / A. L. E. M. Jamel // *Journal of the College of Education for Women*. – 2011. – Vol. 22, No. 3. – P. 627–637.

34. Fractal coding and analysis group [Electronic resource]. – Access mode: <https://links.uwaterloo.ca/Repository/TIF>. – 15.12.2021.

35. USC-SIPI. The USC-SIPI image database [Electronic resource]. – Access mode: <http://sipi.usc.edu/database/database.php?volume=aerials>. – 18.12.2021.

36. Bae, S. A DCT-based total JND profile for spatiotemporal and foveated masking effects [Text] / S. Bae, M. Kim // *IEEE Transactions on Circuits Systems for Video Technology*. – 2016. – Vol. 27, No. 6. – P. 1196–1207. DOI: 10.1109/TCSVT.2016.2539862.

37. Bavirisetti, D. P. Image Fusion Datasets [Electronic resource] / D. P. Bavirisetti. – Access mode: <https://sites.google.com/view/durgaprasadbavirisetti/datasets>. – 11.12.2021.

References (BSI)

1. Zappavigna, M. Social media photography: construing subjectivity in Instagram images, *Visual Communication*, 2016, vol. 15, no. 3, pp. 271–292. DOI: 10.1177/1470357216643220.

2. Stoyanov, D., Taylor, Z. A., Aylward, S. R., Tavares, J. M., Xiao, Y., Simpson, A. L., Martel, A. L., Maier-Hein, L., Li, S., Rivaz, H., Reinertsen, I., Chabanas, M., Farahani, K., Engenharia, F. D. *Simulation, image processing, and ultrasound systems for assisted diagnosis and navigation*. Cham, Springer, 2018. 204 p. DOI: 10.1007/978-3-030-01045-4.

3. Koungianos, E., Mohanty, S. P., Coelho, G., Albalawi, U., Sundaravadivel, P. Design of a high-performance system for secure image communication in the internet of things, *IEEE Access*, 2016, vol. 4, pp. 1222–1242. DOI: 10.1109/ACCESS.2016.2542800.

4. Sayood, K. *Introduction to data compression*. San Francisco, Morgan Kaufmann Publ., 2017. 768 p.

5. Hussain, A. J., Al-Fayadh, A., Radi, N. Image compression techniques: A survey in lossless and lossy algorithms, *Neurocomputing*, 2018, vol. 300, pp. 44–69. DOI: 10.1016/j.neucom.2018.02.094.

6. Telles, J., Kemper, G. A Multispectral Image Compression Algorithm for Small Satellites Based on Wavelet Subband Coding. *Proceedings of the 5th Brazilian Technology Symposium "Smart Innovation, Systems and Technologies"*. Campinas, 2019, pp. 181–191. DOI: 10.1007/978-3-030-57548-9_17.

7. Uchaev, Dm. V., Uchaev, D. V. Theory and methodology of multifractal interpretation of aerospace images. *Proceedings of Twelfth International Conference on Machine Vision (ICMV 2019)*. Amsterdam, 2019, pp. 902–909. DOI: 10.1117/12.2559168.

8. Aiazzi, B., Alparone, L., Baronti, S., Lastrì, C., Selva, M. Spectral distortion in lossy compression of hyperspectral data, *Journal of Electrical Computer Engineering*, 2012, vol. 2012. 8 p. DOI: 10.1155/2012/850637.

9. Ayoobkhan, M. U. A., Chikkannan, E., Ramakrishnan, K. Lossy image compression based on

prediction error and vector quantisation, *EURASIP Journal on Image Video Processing*, 2017, vol. 2017, no. 1, pp. 1–13. DOI: 10.1186/s13640-017-0184-3.

10. Qin, C., Zhou, Q., Cao, F., Dong, J., Zhang, X. Flexible lossy compression for selective encrypted image with image inpainting, *IEEE Transactions on Circuits Systems for Video Technology*, 2018, vol. 29, no. 11, pp. 3341–3355. DOI: 10.1109/TCSVT.2018.2878026.

11. Grgic, M., Kunt, M., Mrak, M. *High-Quality Visual Experience: Creation, Processing and Interactivity of High-Resolution and High-Dimensional Video Signals*. Cham, Springer Publ., 2010. 561 p.

12. Zabala, A., Pons, X., Díaz-Delgado, R., Garcia, F., Auli-Llinas F., Serra-Sagrista, J. Effects of JPEG and JPEG2000 lossy compression on remote sensing image classification for mapping crops and forest areas. *Proceedings of 2006 IEEE International Symposium on Geoscience and Remote Sensing*. Denver, 2006, pp. 790–793. DOI: 10.1109/IGARSS.2006.203.

13. Koschan, A., Abidi, M. Detection and classification of edges in color images. *IEEE Signal Processing Magazine*, 2005, vol. 22, no. 1, pp. 64–73. DOI: 10.1109/MSP.2005.1407716.

14. Ozah, N., Kolokolova, A. Compression improves image classification accuracy. *Proceedings of Canadian Conference on Artificial Intelligence*, 2019, vol. 11489C, pp. 525–530. DOI: 10.1007/978-3-030-18305-9_55.

15. Doss, S., Pal, S., Akila, D., Jeyalakshmi, S., Nusrat Jabeen, T., Suseendran, G. Satellite image remote sensing for identifying aircraft using SPIHT and NSCT. *Journal of Critical Reviews*, 2020, vol. 7, no. 5, pp. 631–634. DOI: 10.31838/jcr.07.05.130.

16. Oh, H., Bilgin, A., Marcellin, M. Visually lossless JPEG 2000 for remote image browsing. *Information*, 2016, vol. 7, no. 3, article no. 45. DOI: 10.3390/info7030045.

17. Yee, D., Soltaninejad, S., Hazarika, D., Mbuyi, G., Barnwal, R., Basu, A. Medical image compression based on region of interest using better portable graphics (BPG). *Proceedings of 2017 IEEE international conference on Systems, Man, and Cybernetics (SMC)*. Banff, 2017, pp. 216–221. DOI: 10.1109/SMC.2017.8122605.

18. Pandey, A., Singh Saini, B., Singh, B., Sood, N. Quality controlled ECG data compression based on 2D discrete cosine coefficient filtering and iterative JPEG2000 encoding. *Measurement*, 2020, vol. 152, article no. 107252. DOI: 10.1016/j.measurement.2019.107252.

19. Liu, H., Zhang, Y., Zhang, H., Fan, C., Kwong, S., Kuo, C.-C. J., Fan, X. Deep learning-based picture-wise just noticeable distortion prediction model for image compression. *IEEE Transactions on Image Processing*, 2019, vol. 29, pp. 641–656. DOI: 10.1109/TIP.2019.2933743.

20. Li, F., Krivenko, S., Lukin, V. A Two-step Procedure for Image Lossy Compression by ADCTC With a Desired Quality. *Proceedings of 2020 IEEE 11th*

International Conference on Dependable Systems, Services and Technologies (DESSERT). Kyiv, 2020, pp. 307–312. DOI: 10.1109/DESSERT50317.2020.9125000.

21. Li, F., Krivenko, S., Lukin, V. A Two-step Approach to Providing a Desired Visual Quality in Image Lossy Compression. *Proceedings of 2020 IEEE 15th International Conference on Advanced Trends in Radioelectronics, Telecommunications and Computer Engineering (TCSET)*. Lviv-Slavske, 2020, pp. 502–506. DOI: 10.1109/TCSET49122.2020.235483.

22. Li, F., Krivenko, S., Lukin, V. Analysis of two-step approach for compressing texture images with desired quality. *Aviaciono-kosmicna tehnika i tehnologia – Aerospace technic and technology*, 2020, no. 1(161), pp. 50–58. DOI: 10.32620/akt.2020.1.08.

23. Li, F., Krivenko, S., Lukin, V. An Approach to Better Portable Graphics (BPG) Compression with Providing a Desired Quality. *Proceedings of 2020 IEEE 2nd International Conference on Advanced Trends in Information Theory (ATIT)*. Kyiv, 2020, pp. 13–17. DOI: 10.1109/ATIT50783.2020.9349289.

24. Li, F., Krivenko, S., Lukin, V. Adaptive two-step procedure of providing desired visual quality of compressed image. *Proceedings of Proceedings of the 2020 4th International Conference on Electronic Information Technology and Computer Engineering*. Xiamen, 2020, pp. 407–414. DOI: 10.1145/3443467.3443791.

25. Li, F., Krivenko, S., Lukin, V. Two-step providing of desired quality in lossy image compression by SPIHT. *Radioelektronni i komp'uterni sistemi – Radioelectronic and computer systems*, 2020, no. 2(94), pp. 22–32. DOI: 10.32620/reks.2020.2.02.

26. Said, A., Pearlman, W. A new, fast, and efficient image codec based on set partitioning in hierarchical trees. *IEEE Transactions on Circuits and Systems for Video Technology*, 1996, vol. 6, no. 3, pp. 243–250. DOI: 10.1109/76.499834.

27. Rao, G. S., Rani, M. L. P., Rao, B. P. Comparative Analysis of SVD and Progressive SPIHT techniques for Compression of MRI and CT Images. *Proceedings of International Conference on Sustainable Computing in Science, Technology & Management (SUSCOM-2019)*, Jaipur, India, 2019, pp. 521–529. DOI: 10.2139/ssrn.3352392.

28. Kumar, B. B. S., Satyanarayana, P. S. Correlative Analysis of EZW and SPIHT Compression

Algorithms using Sevenlets Wavelet Technique. *International Journal of Innovative Technology and Exploring Engineering*, 2020, vol. 9, no. 5, pp. 1099–1104. DOI: 10.35940/ijitee.e2672.039520.

29. Arunpandian, S., Dhenakaran, S. S., An effective image compression technique based on burrows wheeler transform with set partitioning in hierarchical trees. *Concurrency and Computation. Practice and Experience*, 2021, vol. 34, no. 5, article no. e6705. DOI: 10.1002/cpe.6705.

30. Ieremeiev, O., Lukin, V., Okarma, K. Combined Visual Quality Metric of Remote Sensing Images Based on Neural Network. *Radioelectronic and computer systems*, 2020, no. 4, pp. 4–15. DOI: 10.32620/reks.2020.4.01.

31. Li, F., Krivenko, S., Lukin, V. A Fast Method for Visual Quality Prediction and Providing in Image Lossy Compression by SPIHT. *Proceedings of Conference on Integrated Computer Technologies in Mechanical Engineering–Synergetic Engineering*. Kharkov, 2020, pp. 17–29. DOI: 10.1007/978-3-030-66717-7_2.

32. Krivenko, S., Li, F., Lukin, V., Vozel, B., Krylova, O. Prediction of visual quality metrics in lossy image compression. *Proceedings of 2020 IEEE 40th International Conference on Electronics and Nanotechnology (ELNANO)*. Kyiv, 2020, pp. 478–483. DOI: 10.1109/ELNANO50318.2020.9088819.

33. Jamel, A. L. E. M. Efficiency Spiht in compression and quality of image. *Journal of the College of Education for Women*, 2011, vol. 22, no. 3, pp. 627–637.

34. *Fractal coding and analysis group*. Available at: <https://links.uwaterloo.ca/Repository/TIF> (Accessed 15.12.2021).

35. USC-SIPI. *The USC-SIPI image database*. Available at: <http://sipi.usc.edu/database/database.php?volume=aerials> (Accessed 18.12.2021).

36. Bae, S.-H., Kim, M. A DCT-based total JND profile for spatiotemporal and foveated masking effects. *IEEE Transactions on Circuits Systems for Video Technology*, 2016, vol. 27, no. 6, pp. 1196–1207. DOI: 10.1109/TCSVT.2016.2539862.

37. Bavirisetti, D. P. *Image Fusion Datasets*. Available at: <https://sites.google.com/view/durgaprasadbavirisetti/datasets> (Accessed 11.12.2021).

Надійшла до редакції 11.01.2022, розглянута на редколегії 16.02.2022

АДАПТИВНИЙ ДВОЕТАПНИЙ МЕТОД ЗАБЕЗПЕЧЕННЯ БАЖАНОЇ ВІЗУАЛЬНОЇ ЯКОСТІ ДЛЯ SPIHT

Ф. Лі

Стиснення з втратами широко використовується в різних додатках завдяки змінному коефіцієнту стиснення. Однак неминуче вносяться спотворення, і це знижує якість зображення. Таким чином, часто потрібно контролювати якість стиснутих зображень. Нещодавно було запропоновано двоетапний метод для забезпечення бажаної візуальної якості. Осереднена крива коефіцієнт стиснення/ спотворення використана для визначення правильного значення параметра, що контролює стиснення. Однак ефективність підходу для вейвлетного кодера Set Partitioning in Hierarchical Trees (SPIHT) є недостатньою, оскільки існують дуже широкі межі варіації візуальної якості для різних зображень для фіксованого значення параметра, що керує стисненням. Крім того, попередня робота продемонструвала, що рівень помилок, що є предметом нашого

дослідження, є пов'язаним з текстурними особливостями зображення, яке потрібно стиснути, де наявність текстури є невід'ємною властивістю зображень дистанційного зондування. У цій роботі нашою метою є розробити адаптивний двоетапний метод для підвищення точності для SPIHT. Вирішуються наступні задачі. По-перше, виконується прогнозування візуальної якості для певного значення параметра. Схема прогнозування базується на видобуванні інформації з певної кількості блоків для оцінювання візуальної якості для зображення, що стискається із заданим значенням параметру, який контролює стиснення. Для групування за складністю використовується поріг; зображення розділяються на дві групи: прості та складні. По-друге, за результатом групування обирається модельна крива. Нарешті, згідно з цією кривою застосовується двоетапне стиснення. Для оцінки якості зображення використовується класична метрика – пікове відношення сигнал/шум (PSNR). Метод дослідження базується на експерименті для набору зображень, що охоплює різну складність і особливості текстури, проводиться перевірочний експеримент. **Результати** порівняння для чотирьох типових бажаних значень доводять, що точність загалом підвищена, середньоквадратична похибка як першого, так і другого етапів значно зменшена. Середня абсолютна похибка також зменшена. **Висновок:** ефект покращення є значним, особливо при низькій бажаній візуальній якості. Зображення дистанційного зондування береться як приклад для детального аналізу; якість розпакованих зображень відповідає візуальним вимогам користувачів і помилки є допустимими.

Ключові слова: двоетапний підхід; стиснення з втратами; бажана якість; модель адаптивної кривої.

АДАПТИВНИЙ ДВУЕТАПНИЙ МЕТОД ОБЕСПЕЧЕННЯ ЖЕЛАТЕЛЬНОГО ВИЗУАЛЬНОГО КАЧЕСТВА ДЛЯ SPIHT

Ф. Ли

Сжатие с потерями широко используется в разных приложениях благодаря изменяющемуся коэффициенту сжатия. Однако неизбежно вносятся искажения, и это снижает качество изображения. Таким образом, часто следует контролировать качество сжатых изображений. Недавно был предложен двухэтапный метод для обеспечения желаемого визуального качества. Усредненная кривая коэффициент сжатия/искажения использована для определения правильного значения параметра, контролирующего сжатие. Однако эффективность подхода для вейвлетного кодера Set Partitioning in Hierarchical Trees (SPIHT) недостаточна, поскольку существуют очень широкие пределы вариации визуального качества для различных изображений для фиксированного значения параметра, управляющего сжатием. Кроме того, предыдущая работа продемонстрировала, что уровень ошибок, являющийся предметом нашего исследования, связан с текстурными особенностями изображения, которое нужно сжать, где наличие текстуры является неотъемлемым свойством изображений дистанционного зондирования. В данной работе нашей целью является разработать адаптивный двухэтапный способ для повышения точности для SPIHT. Решаются следующие задачи. Во-первых, производится прогнозирование визуального качества для определенного значения параметра. Схема прогнозирования базируется на извлечении информации из определенного количества блоков для оценки визуального качества для сжимаемого изображения с заданным значением параметра, который контролирует сжатие. Для группировки по сложности используется порог; изображения делятся на две группы: простые и сложные. Во-вторых, по результату группировки выбирается модельная кривая. Наконец, согласно этой кривой, применяется двухэтапное сжатие. Для оценки качества изображения используется классическая метрика – пиковое отношение сигнал/шум (PSNR). Метод исследования базируется на эксперименте для набора изображений, охватывающих разную сложность и особенности текстуры, проводится проверочный эксперимент. **Результаты** сравнения для четырех типичных желаемых значений доказывают, что точность в целом повышена, среднеквадратичная погрешность как первого, так и второго этапов значительно уменьшена. Средняя абсолютная погрешность также уменьшена. **Вывод:** эффект улучшения значительный, особенно при низком желаемом визуальном качестве. Изображение дистанционного зондирования берется в качестве примера для детального анализа; качество распакованных изображений соответствует визуальным требованиям пользователей и ошибки допустимы.

Ключевые слова: двухэтапный подход; сжатие с потерями; желаемое качество; модель адаптивной кривой.

Фанфан Ли – аспирантка кафедри інформаційно-комунікаційних технологій імені О. О. Зеленського, Національний аерокосмічний університет «Харківський авіаційний інститут», Харків, Україна; старший викладач лабораторії неруйнівного контролю (Міністерство освіти), Наньчанський аерокосмічний університет, Наньчан, Китай.

Fangfang Li – PhD student of Dept. of Information and communication technologies named after A. A. Zelensky, National Aerospace University «Kharkov Aviation Institute», Kharkiv, Ukraine; Senior Lecturer, Key Laboratory of Nondestructive Testing (Ministry of Education), Nanchang Hangkong University, Nanchang, China, e-mail: liff_niat@sohu.com, ORCID: 0000-0002-7392-586X, Scopus Author ID: 57211096654, ResearchGate: Li_Fangfang3.444.